Environmental Science Advances

ROYAL SOCIETY OF CHEMISTRY

PAPER

View Article Online
View Journal | View Issue

Cite this: *Environ. Sci.: Adv.*, 2022, **1**, 192

Removal of persistent textile dyes from wastewater by Fe(II)/H_2O_2/H_3NOH^+ integrated system: process performance and limitations†

Slimane Merouani, *[a] Aissa Dehane,[a] Aouattef Belghit,[a] Oualid Hamdaoui,[b] Nour El Houda Boussalem[a] and Hassina Daif[a]

With the objective of establishing an overview of the limits of hydroxylamine-induced acceleration of the Fenton process, the impact of a wide range of processing conditions and water matrix compositions (water quality) on the degradation of persistent textile dyes is revealed in this study. The co-use of Fenton reagents and hydroxylamine in its protonated form (H_3NOH^+) enabled the rapid removal of dyes, with a yield improvement of more than 40% compared to the not using H_3NOH^+. H_3NOH^+ broadened the Fenton working pH up to pH 5, where higher degradation efficacy is achieved to that at pH 3. The gap between the Fenton-H_3NOH^+ and Fenton systems in term of dye removal increases with increasing dosages of reactants (*i.e.*, H_3NOH^+, H_2O_2, Fe(II) and dye) and solution pH (2–5). While sulfate and nitrite ions (up to 10 mM) did not affect the efficiency of the process in the presence or absence of H_3NOH^+, chloride greatly hindered the Fenton process (60%) while minimally affecting dye removal by the Fenton-H_3NOH^+ system. The Fenton-H_3NOH^+ system maintained better degradation performance for the breakdown of Basic Fuchsin (BF) in natural mineral water and treated wastewater. However, the degradation efficiencies in sea and river waters are substantially reduced, with just 61 and 58% elimination being reached, respectively. However, the ternary system outperforms the Fenton process alone in all of the studied water matrices. The findings of this work broaden our understanding of the application of hydroxylamine in the Fenton process and highlight the limitations of its influence in boosting the breakdown efficiency of textile dye contaminants.

Received 18th January 2022
Accepted 21st March 2022

DOI: 10.1039/d2va00011c

rsc.li/esadvances

Environmental significance

The main disadvantage of the Fenton system is the buildup and precipitation of Fe(III), which may lead to a further decrease in reaction rates and a narrowing of the optimum pH interval. Hydroxylamine (HA) can overcome these limitations through its rapid reduction of the accumulated Fe(III), which substantially improves the efficiency of the Fenton process. The process conditions and the quality of the water matrix can significantly affect the positive effect of hydroxylamine toward the Fenton process. To establish an overview of the limits of hydroxylamine-induced acceleration of the Fenton process, the impact of a wide range of processing conditions and water matrix compositions (water quality) on the degradation of persistent textile dyes is revealed in this study.

I. Introduction

Colored water is multicomponent wastewater that contains a variety of contaminants. Such wastewater has an intense color, high amounts of total dissolved solids (TDS), high chemical oxygen demand (COD), highly fluctuating pH (2–12), and low biodegradability.[1] The degradation of textile wastewaters is a priority due to the severe problems related to these effluents.[2] Synthetic dye compounds commonly produce more persistent and hazardous species due to the biotic and abiotic changes that occur in wastewater, or they can carry on through the wastewater treatment plant process and have toxic effects on aquatic systems.[3] As a result, specific treatment technologies must be applied to eliminate such chemicals that are difficult to remove by the conventional wastewater treatment chain.

Fenton's reagent (H_2O_2, Fe(II)), initially described over a century ago,[4] produces highly reactive $^{\bullet}OH$ radicals ($E^0 = 2.8$ V/NHE) to begin a radical reactions chain (eqn (1)–(8)),[5,6] and destroys a variety of organic pollutants in water and soil[7–13] with high reaction rate constants of 10^8 to 10^{11} M^{-1} s^{-1}.[14] The Fenton process is the oldest advanced oxidation process.

[a]*Laboratory of Environmental Process Engineering, Department of Chemical Engineering, Faculty of Process Engineering, University Salah Boubnider-Constantine 3, P. O. Box 72, 25000 Constantine, Algeria. E-mail: s.merouani@yahoo.fr; s.merouani03@gmail.com*

[b]*Chemical Engineering Department, College of Engineering, King Saud University, P. O. Box 800, 11421 Riyadh, Saudi Arabia*

† Electronic supplementary information (ESI) available. See https://doi.org/10.1039/d2va00011c

$$Fe(II) + H_2O_2 \rightarrow {}^{\bullet}OH + Fe(III) + OH^-,\ k_1 = 63\text{–}76\ M^{-1}\ s^{-1} \quad (1)$$

$$Fe(III) + H_2O_2 \rightarrow Fe(II) + HO_2^{\bullet} + H^+,\quad k_2 = 0.01 - 0.02\ M^{-1}\ s^{-1} \quad (2)$$

$$^{\bullet}OH + H_2O_2 \rightarrow HO_2^{\bullet} + H_2O,\quad k_3 = (1.2 - 4.5) \times 10^7\ M^{-1}\ s^{-1} \quad (3)$$

$$Fe(II) + {}^{\bullet}OH \rightarrow Fe(III) + OH^-,\ k_4 = (3\text{–}4.3) \times 10^8\ M^{-1}\ s^{-1} \quad (4)$$

$$Fe(III) + HO_2^{\bullet} \rightarrow Fe(II) + O_2 + H^+,\quad k_5 = (0.1 - 3.1) \times 10^5\ M^{-1}\ s^{-1} \quad (5)$$

$$Fe(II) + HO_2^{\bullet} + H^+ \rightarrow Fe(III) + H_2O_2,\quad k_6 = 1.2 \times 10^6\ M^{-1}\ s^{-1} \quad (6)$$

$$^{\bullet}OH + {}^{\bullet}OH \rightarrow H_2O_2,\ k_7 = (4.2\text{–}5.5) \times 10^9\ M^{-1}\ s^{-1} \quad (7)$$

$$HO_2^{\bullet} + HO_2^{\bullet} \rightarrow H_2O_2 + O_2,\quad k_8 = 8.3 \times 10^5\ M^{-1}\ s^{-1} \quad (8)$$

Nonetheless, the Fenton system has certain inherent disadvantages that restrict its broad applicability, such as tight pH range constraints, high H_2O_2 dose, and the buildup of ferric oxide sludge, which causes oxidation rates to drop and necessitates an additional separation stage.[3,9] To prevent precipitation of iron as hydroxide, the Fenton reaction must always be conducted under acidic conditions (pH 3–4).[9] The reaction shows its highest catalytic performance around pH 3, beyond which its effectiveness declines.[15]

The principal disadvantage of the Fenton system is the buildup and precipitation of ferric iron. Some reductants with a weak reaction rate with $^{\bullet}OH$ radicals might reduce Fe(III) to Fe(II), which has greater solubility than ferric iron. Hydroxylamine (HA) can play this role. HA has two pK_a values of 5.96 and 13.74.[16] The protonated form of hydroxylamine (H_3NOH^+) is dominant for pH < 5, whereas the non-protonated form (NH_2OH) is the major form between pH 7 and 12. H_3NOH^+ and H_2NOH react with $^{\bullet}OH$ at rate constants of $\leq 5.0 \times 10^8\ M^{-1}\ s^{-1}$ and $9.5 \times 10^9\ M^{-1}\ s^{-1}$, respectively,[16] so the scavenging of $^{\bullet}OH$ by hydroxylamine increases with an increase in pH. According to Chen *et al.*,[17] hydroxylamine may efficiently accelerate the redox cycle of Fe(III) to Fe(II), resulting in relatively steady Fe(II) recovery, thus increasing the reaction rates and expanding the operable pH range up to 5.7. Hydroxylamine exhibited significant promotion of the degradation of benzoic acid, tartrazine and glycerin by the Fenton system.[18–20] The same statement has been proven by Liu *et al.*[21] and Zou *et al.*[22] when the degradation of sulfamethoxazole and benzoic acid was carried out with Fe(II)/$HOSO_5^-$ (*i.e.*, a sulfate radical-based AOP) in the presence of hydroxylamine. Both $SO_4^{\bullet -}$ radicals and $^{\bullet}OH$ radicals were considered the primary reactive oxidants for the degradation of sulfamethoxazole and benzoic acid in the Fe(II)/$HOSO_5^-$–H_3NOH^+ process, as confirmed by experiments with electron spin trapping and alcohol quenching tests.[21,22] Additionally, NO_3^- and N_2O were the dominant products of hydroxylamine degradation in the Fenton process.[17] Other studies have reported N_2, N_2O, NO_3^- and NO_2^- as the final products of Fe(III) reduction by hydroxylamine and provided the following reaction pathways:[17,18,21–25]

$$Fe(III) + H_3NOH^+ \rightleftharpoons Fe(H_2NOH)^{3+} + H^+,\ k_9 = 6.88 \times 10^7\ M^{-1}\ s^{-1},\ k_{-9} = 9.42 \times 10^{10}\ M^{-1}\ s^{-1} \quad (9)$$

$$Fe(H_2NOH)^{3+} + H^+ \rightleftharpoons Fe(II) + H_2NO^{\bullet} + H^+,\ k_{10} = 5.97 \times 10^5\ M^{-1}\ s^{-1},\ k_{-10} = 1.67 \times 10^{11}\ M^{-1}\ s^{-1} \quad (10)$$

$$Fe(III) + H_2NO^{\bullet} \rightarrow Fe(II) + NHO + H^+ \quad (11)$$

$$^{\bullet}OH + H_3NOH^+ \rightarrow H_2NO^{\bullet} + H_2O + H^+,\quad k_{12} < 5.0 \times 10^8\ M^{-1}\ s^{-1} \quad (12)$$

$$NHO + H_3NOH^+ \rightarrow N_2 + 2H_2O + H^+ \quad (13)$$

$$H_2NO^{\bullet} + {}^{\bullet}OH \rightarrow NHO + H_2O \quad (14)$$

$$H_2NO^{\bullet} + H_2NO^{\bullet} \rightarrow N_2 + 2H_2O,\ k_{15} = 2.8 \times 10^8\ M^{-1}\ s^{-1} \quad (15)$$

$$NHO + NHO \rightarrow N_2O + H_2O,\ k_{16} = (4.5 \pm 2.7) \times 10^9\ M^{-1}\ s^{-1} \quad (16)$$

$$5Fe(III) + 2H_2O + H_2NO^{\bullet} \rightarrow N_3O^- + 6H^+ + 5Fe(II),\ k_{17} = n/a \quad (17)$$

$$N_3O^- + H_2NOH + OH^- \rightarrow NO^- + N_2O^- + H_2O,\ k_{18} = n/a \quad (18)$$

Even though the accelerating effect of hydroxylamine on the efficiency of the Fenton system is well established,[17–22,24,25] as stated above, the limits of the accelerating effect have not been well demonstrated, particularly when pollutant degradation is carried out in water matrices other than deionized water. The process conditions and the quality of the water matrix are the main factors controlling the positive effect of hydroxylamine toward the efficiency of the Fe(II)/H_2O_2 process. In fact, due to its strong reducing effect, hydroxylamine can be strongly consumed by minerals and natural organic matter existing in real environmental matrices, thereby limiting its ability to regenerate Fe(II), which could inhibit the effectiveness of the Fenton process. Therefore, knowing the limits of the enhancing effect of hydroxylamine toward the efficiency of the Fenton process means establishing a phase diagram for the Fe(II)/H_2O_2/hydroxylamine ternary system, which is a very important issue.

The current work aims to broaden knowledge in this field by investigating the sensitivity of the Fenton-H_3NOH^+ process to the presence of mineral water constituents, *i.e.*, salts and natural organic materials. The process efficiency was assessed in a variety of water matrices, including natural mineral water, seawater, river water and secondary effluent from a wastewater treatment plant. All these degradation data were conducted, in parallel, without H_3NOH^+ (with the traditional Fenton process) with the objective of establishing an overview of the limits of hydroxylamine accelerating pollutant degradation by the Fenton process (a phase diagram vision for the Fe(II)/H_2O_2/H_3NOH^+ process). Five textile dyes (*i.e.*, Basic Fuchsin, Chlorazol Black, Safranin O, Rhodamine B and Light Green SF Yellowish) of confirmed persistence and carcinogenicity were chosen as substrate models.[26–30] Fenton-H_3NOH^+ was used in

this study and tested under various real situations of textile wastewater.

2. Material and methods

2.1. Reagents

All of the chemicals were reagent grade and were utilized without additional purification. The dyes Basic Fuchsin (BF, MW: 337.84 g mol^{-1}, class: *triphenylmethane*), Rhodamine B (RhB, MW: 479.01 g mol^{-1}, class: *xanthene*), Chlorazol Black (CB, MW: 781.73 g mol^{-1}, class: *azo*), Safranin O (SO, MW: 350.85 g mol^{-1}, class: *quinone-imine*) and Light Green SF Yellowish (LGSFW, MW: 792.85 g mol^{-1}, class: *triarylmethane*), selected as substrates, were purchased form Sigma-Aldrich and used as received. All other chemicals, *i.e.*, hydrogen peroxide (H_2O_2, wt 35%) iron sulfate ($FeSO_4 \cdot 7H_2O$), hydroxylamine hydrochloride (HA: $NH_2OH \cdot HCl$, >99%), sodium chloride (NaCl), sodium sulfate (Na_2SO_4), sodium nitrite ($NaNO_2$), sodium nitrate ($NaNO_3$), sulfuric acid (H_2SO_4, >99%) and sodium hydroxide (NaOH, >99%) were of the purest analytical grade available. All reagent solutions were prepared using deionized water. Fresh solutions of H_2O_2 and hydroxylamine (20 mM) were prepared every day to avoid their self-decomposition over time. Dye stock solutions (500 mg L^{-1}) were prepared in deionized water and kept in the dark by covering the dye-vials with aluminum foil. The Fe(II) stock solution (10 mM) was prepared in acidic water (pH 3).

Mediterranean seawater was gathered from north-eastern Algeria in the autumn of 2021. During the same time period, wastewater samples were withdrawn from the secondary treated effluent (prior to chlorination) of a municipal wastewater treatment plant (SEWTP) located at the city of Constantine, Algeria. The basic parameters of the mineral water, seawater, and SEWTP utilized in this investigation are listed in Table 1. The characteristics of the river water were unknown. Before use in experiments, seawater, SEWTP and river samples were all filtered using a 1 m GA-100 fiber glass filter. The filtrates were then kept in clean containers in a refrigerator (4 °C).

Table 1 Main characteristics (before pH adjustment) of natural mineral water, seawater and SEWTP used in this study

	Mineral water	Seawater	SEWTP[a]
pH	7.4	7.6	7.6
Ca^{2+}	59.0 mg L^{-1}	0.4 g L^{-1}	
Mg^{2+}	45.0 mg L^{-1}	1.3 g L^{-1}	
Na^+	15.0 mg L^{-1}	11.0 g L^{-1}	Salinity = 0.8 g L^{-1}
K^+	2.0 mg L^{-1}	—	
Cl^-	22.0 mg L^{-1}	20.0 g L^{-1}	
SO_4^{2-}	40.0 mg L^{-1}	3.0 g L^{-1}	
HCO_3^-	378.2 mg L^{-1}	—	
Br^-	0	65–80 mg L^{-1}	
COT[b]	0	~1.2–1.5	
COD[c]	0	2.71–4.69 mg L^{-1}	
BOD_5[d]	0	1.78–2.92 mg L^{-1}	13 mg L^{-1}

[a] Secondary effluent of wastewater treatment plant. [b] Total organic carbon. [c] Chemical oxygen demand. [d] BOD_5: biological oxygen demand.

2.2. Experimental setup and procedures

Using 200 mL of the solutions, all experiments were carried out in a cylindrical glass cell with standard laboratory lighting. The cell was kept in a temperature-controlled cylindrical water bath, and the reacting solution was magnetically stirred (300 rpm) from the bottom of the bath. The reaction solutions were prepared by adding specific amounts of hydroxylamine, Fe(III) and each dye into deionized water. The pH of the solution was adjusted using 1 M H_2SO_4 or 1 M NaOH solution to the desired value through a pH-meter (Jenway 3505). The reaction was initiated by adding an aliquot of H_2O_2. The variation in solution pH after adding H_2O_2 was less than 0.1 pH units. Samples were withdrawn at predetermined time intervals and immediately transferred into the quartz cell of a UV-Vis. spectrophotometer (Jenway 6405) to measure the absorbance of dyes at their maximum absorption wavelengths (545 nm for Basic Fuchsin, 578 nm for Chlorazol Black, 518 nm for Safranin O, 551 nm for Rhodamine B and 630 nm for Light Green SF Yellowish). Calibration curves based on the Lambert–Beer equation were used to determine dye concentrations during oxidation runs. All tests were repeated at least three times, and the findings were reported as averages (error bars indicate the 95% confidence interval).

The Fe(III) concentration in the Fe(II)/KPS/H_3NOH^+ system was determined spectrophotometrically, as described by Merouani *et al.*[31] Fe(III) is characterized by a distinguishable band in the UV-region with a maximum wavelength of 300 nm in an aqueous solution. The concentration of Fe(III) was determined with the Beer–Lambert Law (Abs = $\varepsilon L \times C$), where ε (the extinction coefficient of Fe(III)) = 2197 L mol^{-1} cm^{-1} and L (the optical path of the quartz cuvette) = 1 cm.

3. Results and discussion

In the following, we started by first investigating the different operating parameters, *i.e.*, H_3NOH^+, Fe(II), H_2O_2 and pollutant concentrations and initial solution pH on the dye degradation. Then, the effect of various mineral salts was shown. Finally, the effect of the different water matrices was studied. All degradation data were provided for both Fenton (no H_3NOH^+) and Fenton-H_3NOH^+ systems (i) to demonstrate the influence of hydroxylamine in the oxidation processes, (ii) to show the difference in behavior between Fenton and Fenton-H_3NOH^+ processes with respect to operating circumstances, and (iii) to state the dependence of the H_3NOH^+-effect on experimental conditions.

3.1. Effect of the Fe(II)/H_2O_2/H_3NOH^+ ternary system on dye removal

Fig. 1a depicts the effect of the initial H_3NOH^+ dosage (0.01–1 mM) at 25 °C on the kinetics of Basic Fuchsin (BF) degradation in an acidic environment (pH 3) for starting Fe(II) and H_2O_2 concentrations of 0.05 and 0.5 mM, respectively. The oxidation of BF in the Fenton system (0 mM H_3NOH^+) occurs in two stages: a rapid primary stage in which 43% of the BF is removed in the first minute, followed by an overly slow secondary stage in

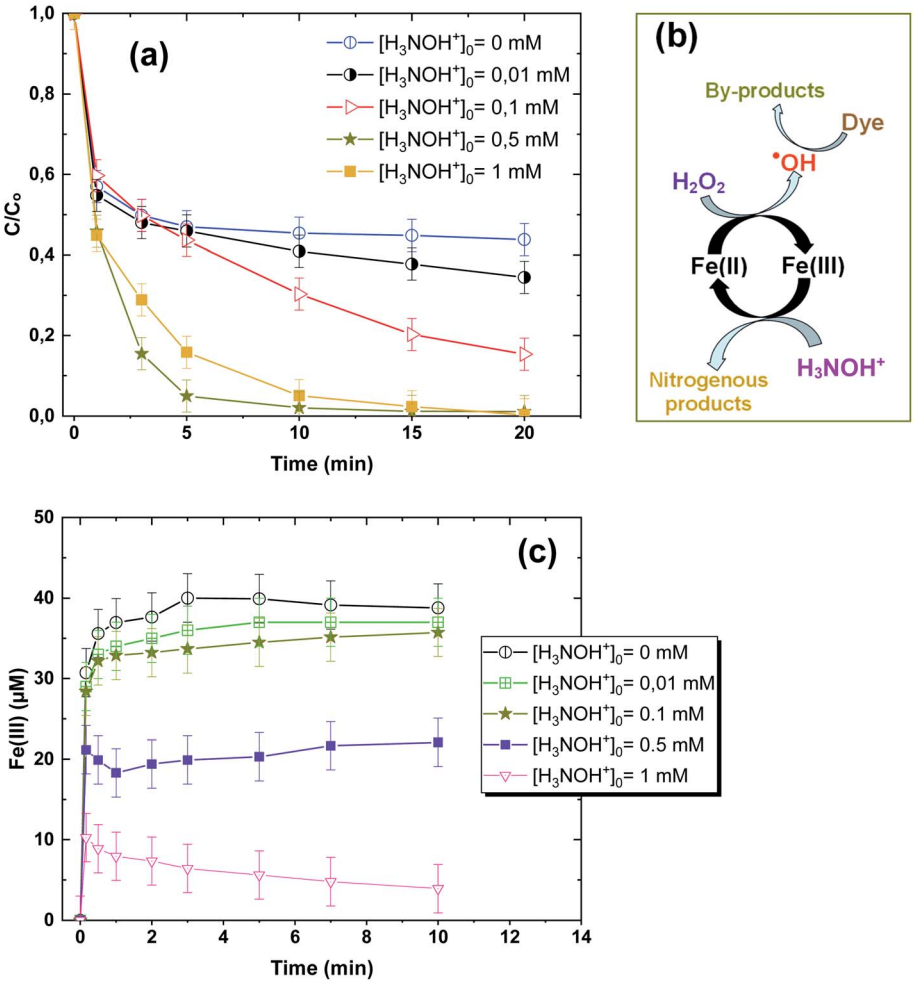

Fig. 1 (a) Effect of initial H_3NOH^+ concentration on the removal kinetics of BF by the system Fe(II)/H_2O_2/H_3NOH^+ (vol. = 200 mL, pH 3, temp. ~25 °C, $C_0 = 20$ μM, $[Fe(II)]_0 = 0.05$ mM, $[H_2O_2]_0 = 0.5$ mM, $[H_3NOH^+]_0 = 0.01$–1 mM). (b) The mechanism of H_3NOH^+-induced enhancement of degradation. (c) Measurement of the Fe(III) formation kinetics in the Fe(II)/H_2O_2 system for the different investigated initial concentrations of H_3NOH^+.

which the dye removal reaches 56% after 20 minutes of reaction. This scenario, which has largely been reported for the Fenton process,[25,32–34] implies that neither the first-order kinetics law nor the second-order law can be ascribed to the kinetics of degradation of the dye by the simple Fenton system. Also, this trend is found to be dependent on the initial Fe(II) concentration and its rate-limiting step (of the fast stage), as shown in eqn (1). The slower second stage is caused by the buildup of Fe(III) and the poor recovery of Fe(II) by reactions (2) and (5), which are significantly slower than reaction (1). Instead, the interaction of Fe(III) with H_2O_2 through eqn (3) produces $HO_2^{\bullet}$, which has a much lower oxidation aptitude than $HO^{\bullet}$.

It has been observed that the presence of H_3NOH^+ significantly improves the efficiency of the Fenton process. BF elimination after 5 minutes of reaction reaches 80 and 95% in the presence of $[H_3NOH^+]_0 = 0.3$ and 0.5 mM, compared to 53% achieved by the Fe(II)/H_2O_2 process, representing a 42% improvement in process efficiency. This is due to the fast reduction of Fe(III) to Fe(II) by H_3NOH^+ (eqn (9), (10), (11) and (17)), which maintains a high level of Fe(II) and then accelerates the generation of $^{\bullet}OH$ radicals through eqn (1). The Fe(II)/H_2O_2/H_3NOH^+ process mechanism is illustrated in Fig. 1b. When an excess of H_3NOH^+ (1 mM) is applied, the removal yield at 5 minutes is 74%, which is less than the yield obtained with 0.5 mM H_3NOH^+ by 21%. Wang *et al.*[25] revealed an optimum H_3NOH^+ dosage of 0.4 mM for the degradation of norfloxacin (10 mg L^{-1}) when using 10 μM of Fe(II) and 1 mM of H_2O_2 at pH 3. This due to the fact that when the optimal concentration (*i.e.*, 0.5 mM) is exceeded, a large amount of $^{\bullet}OH$ radicals could be quenched by the excess of H_3NOH^+ with high rate constant, according to eqn (12). A second alternative phenomenon that may slow down the degradation rate at a higher level of H_3NOH^+ is rapid radical recombination [eqn (7), $k_7 = 5.5 \times 10^9$ M^{-1} s^{-1} and eqn (15), $k_{15} = 2.8 \times 10^8$ M^{-1} s^{-1}], since the concentration of radicals is thought to be higher at higher H_3NOH^+ solution-concentration. Because, as the loading of HA exceeds its optimum (0.5 mM), the quantity of ferrous ions (Fe(II)) and $H_2NO^{\bullet}$ radicals is greatly increased (eqn (9)–(11)). Therefore, according to eqn (15), the amount of $H_2NO^{\bullet}$ radicals is reduced thanks to their accelerated recombination. On the other hand,

eqn (1) indicates that the production of hydroxyl radicals is expedited by the important quantity of ferrous ions formed according to eqn (9)–(11). Consequently, the recombination of $^{\bullet}OH$ radicals is accelerated, which causes the decrease in dye degradation. Different oxidants/species have been found to perform a similar role in several degradation situations involving various $^{\bullet}OH$ or $SO_4^{\bullet-}$-based AOPs.[3,27,35–41] Consequently, an excessive amount of hydroxylamine (>0.5 mM in our case) should be avoided for the best performance of the Fe(II)/H_2O_2/H_3NOH^+ integrated process.

To confirm the above enhancement/quenching mechanism of NH_3OH^+ toward radical generation in the Fe(II)/H_2O_2 system, additional experimental evidence was added by analyzing the Fe(III) production kinetics in the presence of low (0.01, 0.1 mM) and excess amounts of H_3NOH^+ (1 mM) and comparing the obtained evolution with that achieved at 0.5 mM (*i.e.*, the optimal HA concentration, which provided the best improvement in Fe(II)/H_2O_2 efficiency, Fig. 1a). The obtained Fe(III) profiles for 0.01 to 1 mM NH_3OH^+ are plotted in Fig. 1c. As can be seen, a significant reduction in Fe(III) generation is obtained with an increase in $[H_3NOH^+]_0$ from 0.01 to 0.5 mM, indicating a rapid decrease in this species by H_3NOH^+, as has already been stated in the previous paragraph. This trend is accompanied by a parallel rapid increase in the dye removal rate, as shown in Fig. 1a. However, Fig. 1c clearly shows that a further increase in H_3NOH^+ to 1 mM further enhanced the reduction rate of Fe(III), compared to 0.5 mM, which contradicts the trend observed in Fig. 1a, where H_3NOH^+ at 1 mM quenches the degradation of the dye (*i.e.*, no further enhancement in the dye removal rate resulted when the H_3NOH^+ dosage increased from 0.5 to 1 mM). This means that H_3NOH^+, when it exists at a higher concentration (1 mM), does not alter the Fe(III) reduction rate significantly, but it mainly quenches the resulting radicals (existing at higher concentration in this case) as no further augmentation in the degradation efficiency of the dye is obtained when operating with 1 mM of hydroxylamine (Fig. 1a). In parallel to

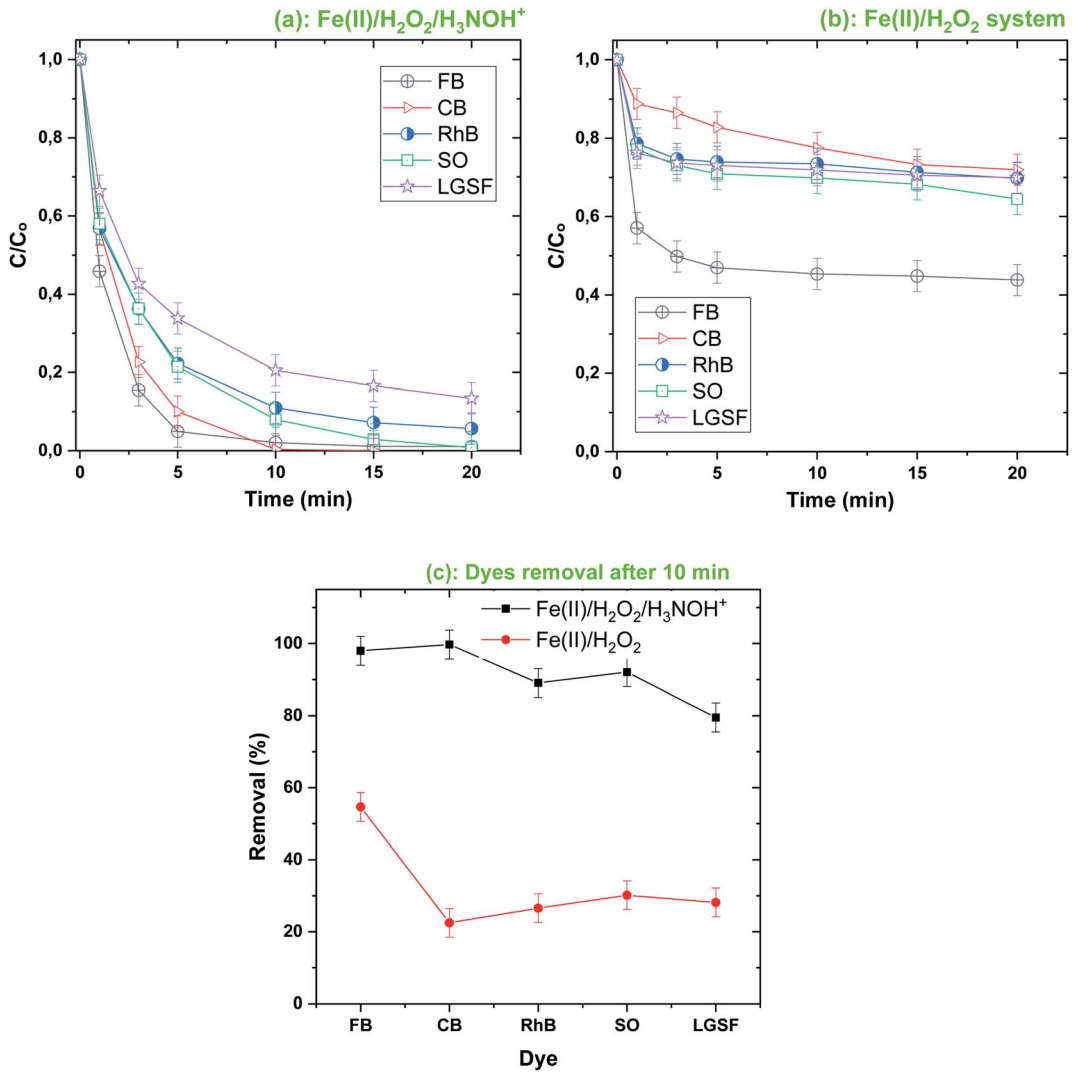

Fig. 2 Comparison of the degradation of different dyes by the Fenton-H_3NOH^+ (a) and the sole Fenton (b) processes, and dyes elimination after 10 min (c) (vol. = 200 mL, pH 3, temp. ~25 °C, C_0 = 20 μM, $[Fe(II)]_0$ = 0.05 mM, $[H_2O_2]_0$ = 0.5 mM, $[H_3NOH^+]_0$ = 0.5 mM). (c) Dye removal (%) at 10 min for both processes (*i.e.* Fenton-H_3NOH^+ and Fenton).

this mechanism, the quenching of radicals by self-recombination (*i.e.*, a parasitic pathway for radical consumption by dyes) may occur due to the higher rate constants of these reactions (eqn (7) and (15)).

The accelerating role of H_3NOH^+ was confirmed for diverse dyes, as demonstrated in Fig. 2, where the removal kinetics of RhB, SO, CB and LGHSY were highly efficient in the Fenton-H_3NOH^+ system compared to the simple Fenton system. Contrary to the Fenton degradation tendency of Fig. 2b (*i.e.*, a fast stage followed by a steady one), the profiles of dye removal in the Fenton-H_3NOH^+ system follow a rapid exponential decrease (Fig. 2a), reflecting the overcoming role of H_3NOH^+ toward the recovery of Fe(II) through the reaction with the accumulated ferric ions. The Fenton-H_3NOH^+ system was more efficient in the cases of CB, RhB, SO and LGSFY than BF. Compared to the Fenton treatment, degradation improvements of 51% for LGSFY, 61% for RhB and SO and 77% for CB were recorded upon Fe(II)/H_2O_2/H_3NOH^+ treatment, against 42% for the case of BF (Fig. 2c).

The evolution of the UV-Vis. spectra of BF during treatment with Fenton and Fenton-H_3NOH^+ at pH 3 is shown in Fig. 3 under the conditions of $[Fe(II)]_0 = 0.05$ mM and $[H_2O_2]_0 = [H_3NOH^+]_0 = 0.5$ mM. The initial spectrum of BF ($t = 0$ min) is characterized by three absorption peaks at 544 nm (from the chromophoric group), 286 nm (from the derivative aromatic rings) and 210 nm (for the aromatic rings). After 1 min of reaction, the absorbance at 544 nm decreased suddenly from 1 to 0.5247 in the Fenton process (~47% decrease) and to 0.353 in the Fenton-H_3NOH^+ process (~64% decrease); the results of which are in total accordance with the concentration profiles of Fig. 1a. For the 210 and 286 bands, no change is observed in the Fenton process during the whole treatment time (Fig. 3a), whereas important declines of 33.3% at 210 nm (the abs. declined from 0.288 to 0.192) and 28% (the abs. declined from 0.497 to 0.358) at 286 nm are recorded in the Fenton-H_3NOH^+ system (Fig. 3b) at 1 min. This reveals an effective cleavage of the aromatic rings of the dye. Therefore, the Fenton-H_3NOH^+ causes a real degradation of the dye rather than simple decolorization as obtained for the first case (Fig. 3a). As time increases, the three absorption bands of Fig. 3b continue to decline progressively upon Fenton-H_3NOH^+ treatment, reaching 100%, 60.7%, and 57.7% reductions at 20 min for 554, 286 and 210 nm, respectively, reflecting the continuous breakage of the aromatic rings of the dye. This indicates that the Fenton-H_3NOH^+ process can successfully accomplish mineralization.

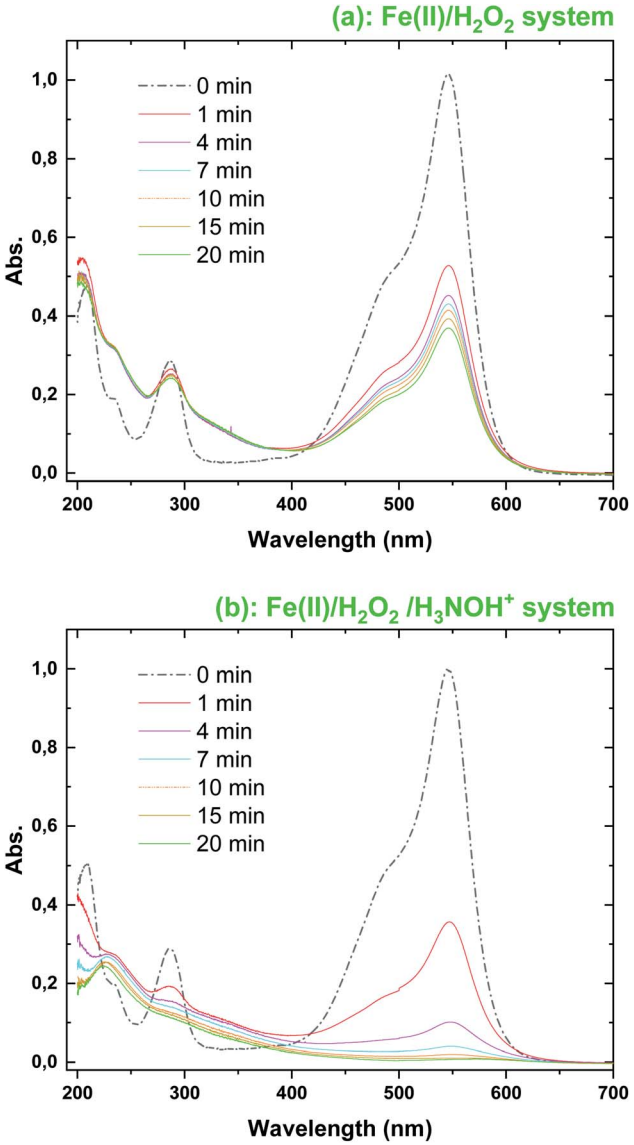

Fig. 3 Evolution with time of the UV-Vis. spectra during the degradation of FB by the (a) Fenton and (b) Fenton-H_3NOH^+ processes (vol. = 200 mL, pH 3, temp. ~25 °C, $C_0 = 20$ μM, $[Fe(II)]_0 = 0.05$ mM, $[H_2O_2]_0 = 0.5$ mM, $[H_3NOH^+]_0 = 0.5$ mM).

3.2. Primary oxidizing species

EPR and chemical probe techniques are usually employed for determining the reactive species involved in AOPs,[3,38,39,42–44] and both of these techniques provided similar results and conclusions.[42,43] Because of the simplicity of the second one (the chemical probe), it has been adopted in the present study.

Identifying $^{\bullet}OH$ radical action with *tert*-butanol (*t*-BuOH) is broadly and routinely used in AOPs. Fig. 4 shows quenching tests using *tert*-butanol (*t*-BuOH: 1–100 mM), which is a strong $^{\bullet}OH$ scavenger ($k_{t\text{-BuOH},^{\bullet}OH} = 7.6 \times 10^8$ M^{-1} s^{-1}), on the competition of $^{\bullet}OH$ with BF dye in the Fenton and Fenton-H_3NOH^+ processes. Degradation profiles of the binary systems H_3NOH^+/Fe(II) and H_3NOH^+/H_2O_2 are also depicted in this figure. Firstly, neither H_3NOH^+ alone nor H_3NOH^+/Fe(II) or H_3NOH^+/H_2O_2 can degrade BF under the given experimental conditions (Fig. 3). Thus, despite the fact that Chen *et al.*[16] reported that hydroxyl radicals can be produced *via* the interaction between H_3NOH^+ and H_2O_2 at pH 3, no evidence has been confirmed herein, which may be due to the low H_2O_2 and H_3NOH^+ loadings utilized in our study (Chen's studies used $[H_2O_2] = [H_3NOH^+] = 10$ mM, whereas our work used $[H_2O_2] = [H_3NOH^+] = 0.5$ mM). As a result, the contributions of the H_3NOH^+/Fe(II) and H_3NOH^+/H_2O_2 systems to the positive impact of the Fenton-H_3NOH^+ process are ruled out. However, adding 1 mM of *t*-BuOH resulted in a complete quenching of the

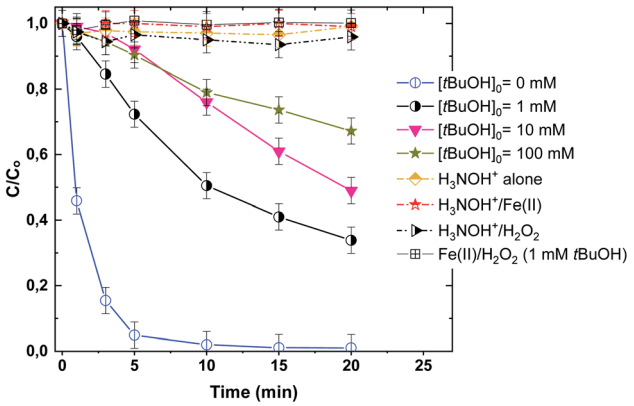

Fig. 4 Effect of *tert*-butanol (*t*-BuOH) on the degradation kinetics of BF by the Fenton-H_3NOH^+ system (vol. = 200 mL, pH 3, temp. ~25 °C, C_0 = 20 μM, $[Fe(II)]_0$ = 0.05 mM, $[H_2O_2]_0$ = 0.5 mM, $[H_3NOH^+]_0$ = 0.5 mM, $[tBuOH]_0$ = 1–100 mM).

Fenton process (Fig. 4), validating the $^{\bullet}OH$-degradation route for the interaction between H_2O_2 and Fe(II). For the case of the Fenton-H_3NOH^+ process, the addition of 1 and 10 mM *t*-BuOH reduces the dye removal at 10 min from 98% (no H_3NOH^+) to 50 and 24%, respectively, but no further important inhibition was seen when $[t\text{-BuOH}]_0$ was raised to 100 mM. These data support the primary role of hydroxyl radicals in dye degradation and show that additional reactive species, probably $H_2NO^{\bullet}$ radicals, may be involved in the dye breakdown because using too much *t*-BuOH, *i.e.*, 100 mM, does not completely quench the BF elimination rate. Chen *et al.*[17] made the same observation for the degradation of benzoic acid (40 M) in a Fenton-H_3NOH^+ process utilizing $[Fe(II)]_0$ = 0.01 mM, $[H_2O_2]_0$ = 0.4 mM, and $[H_3NOH^+]_0$ = 0.4 mM. The involvement of $H_2NO^{\bullet}$ radicals was supported by the main chemical reactions responsible for their generation in addition to ferrous ions (eqn (9)–(11)), where $H_2NO^{\bullet}$ radicals are considered the principal intermediate for Fe(II) recycling.

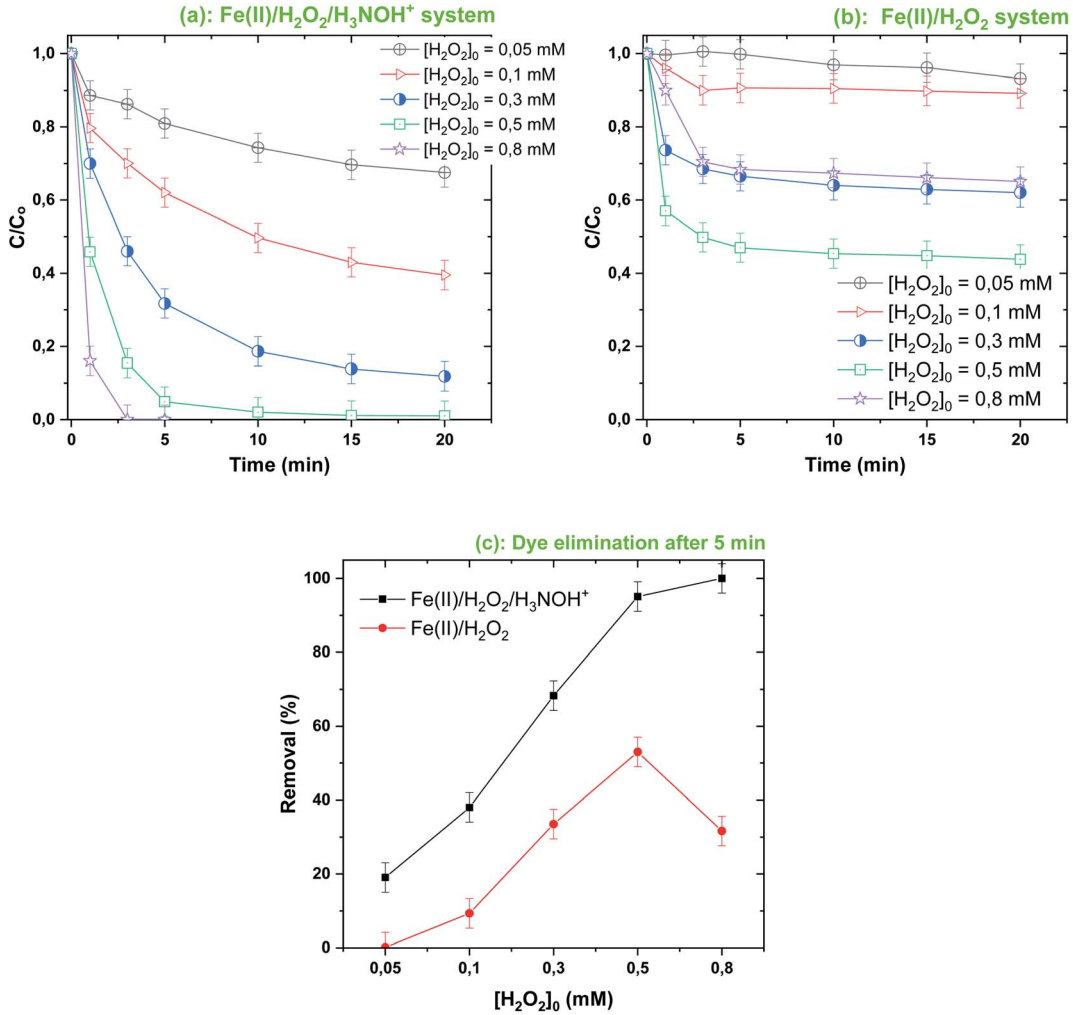

Fig. 5 Effect of $[H_2O_2]_0$ on the degradation kinetics of BF by the Fenton-H_3NOH^+ (a) and the sole Fenton (b) processes, and dye elimination after 5 min (c) (vol. = 200 mL, pH 3, temp. ~25 °C, C_0 = 20 μM, $[Fe(II)]_0$ = 0.05 mM, $[H_2O_2]_0$ = 0.05–0.8 mM, $[H_3NOH^+]_0$ = 0.5 mM).

3.3. Effect of initial Fe(II), H_2O_2 and dye loadings

Fig. 5–7 show the different impacts of initial H_2O_2, Fe(II) and dye concentrations, respectively, on the removal efficiency of BF upon treatment with Fenton-H_3NOH^+ and Fenton systems at pH 3 and 25 °C. In Fig. 5 the concentration of hydrogen peroxide is varied from 0.05 to 0.8 mM for a fixed Fe(II) loading of 0.05 mM, whereas [Fe(II)] was increased up to 0.2 mM for Fig. 6 ($[H_2O_2]_0 =$ 0.5 mM). For the case of the C_0 effect (Fig. 7), H_2O_2, Fe(II) and H_3NOH^+ doses were maintained at 0.5 mM, 0.05 mM and 0.5 mM, respectively.

As can be seen, proportional behavior between the change in Fenton reagent dosages (below 0.05 mM Fe(II) and 0.5 mM H_2O_2) and the dye elimination rate is exhibited for both Fenton and Fenton-H_3NOH^+ systems (Fig. 5–7). However, a disproportional trend is observed for the initial dye concentration effect, where the dye removal was significantly diminished as C_0 increased from 10 to 40 μM (Fig. 7). Besides, the Fenton-H_3NOH^+ process proceeds faster than the Fenton process for all conditions of Fe(II), H_2O_2 and C_0 (Fig. 4–7). The Fenton process exhibits an optimum for 0.5 mM H_2O_2 (Fig. 4b) and 0.1 mM Fe(II) (Fig. 6b), where dye removals of 53% and 70% are achieved, respectively (Fig. 5c and 6c). The corresponding eliminations at these optimum points with the H_3NOH^+-assisted Fenton process are 95% and 97.5%. Interestingly, no optimum H_2O_2 concentration is observed for the latter system where an increase in $[H_2O_2]_0$ from 0.5 mM (the optimum dose for Fenton) to 0.8 mM continuously increases the dye removal from 95 to 100% (Fig. 5c). This does not imply that limitless $[H_2O_2]_0$ may be utilized; nevertheless, an optimal dose ($[H_2O_2]_{0,opt} = 1$ mM) was found by Wang *et al.*[45] for the degradation of Rhodamine B by the system Ce(IV)/H_2O_2/H_3NOH^+ in which cerium(IV) performs the same catalytic function as Fe(II). Similarly, an optimum HSO_5^- (replacement for H_2O_2) was reported by Liu *et al.*[21] in a study investigating the degradation of sulfamethoxazole by the Fe(II)/HSO_5^-/H_3NOH^+ ternary process at pH 5. On the other hand, the same optimum $[Fe(II)]_0$ of 0.1 mM was found for both Fenton and Fenton-H_3NOH^+ processes (Fig. 6a and b). From Fig. 5c and 6c, the largest differences between Fenton-H_3NOH^+ and Fenton in terms of removal efficiency were obtained at 0.8 mM H_2O_2 (Fig. 5c, where the gap is about 70%) and 0.1 mM Fe(II) (Fig. 6c, where the gap is about 43%). Therefore, the Fenton reaction with hydroxylamine results in greater removal efficiency even at higher H_2O_2/Fe(II) concentrations.

Consequently, increasing the Fe(II) or H_2O_2 initial concentration above the optimum dosages can improve the processes efficiency through the same mechanism, *i.e.*, enhancing $^{\bullet}OH$ production *via* reaction (1); however, an excess of these

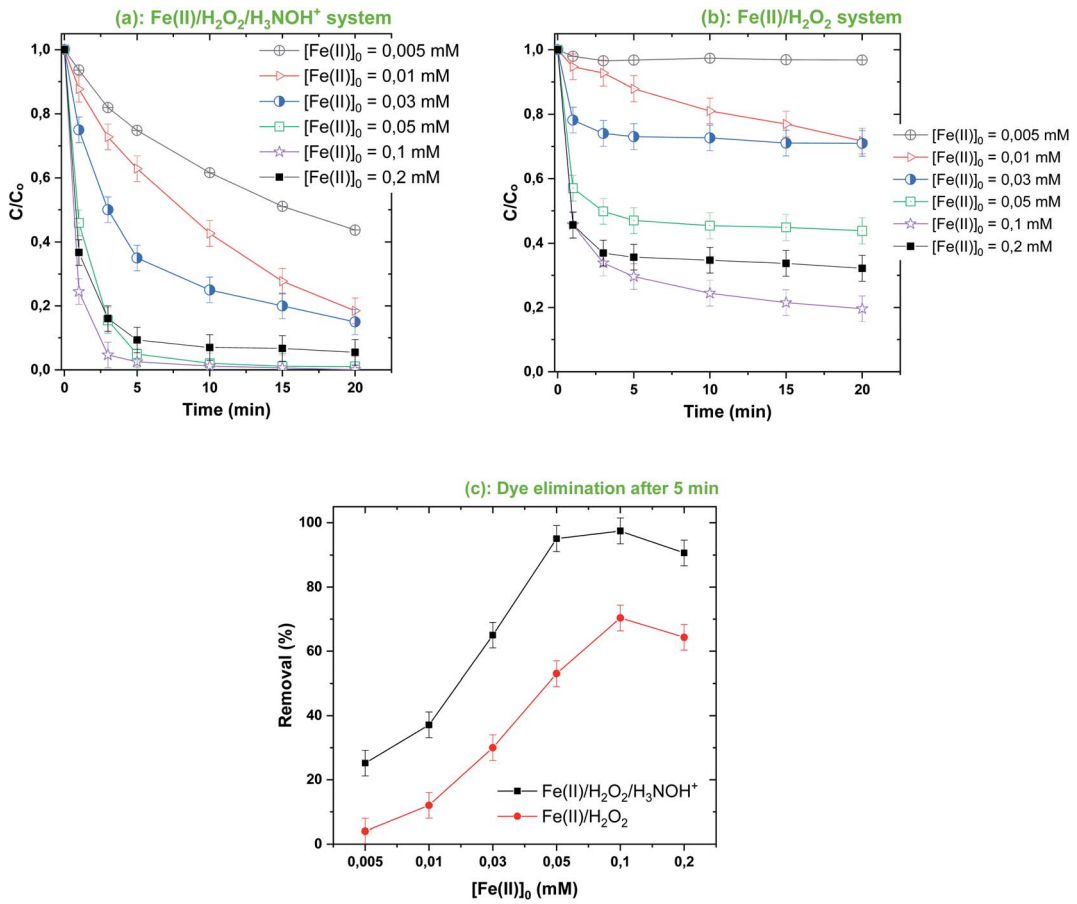

Fig. 6 Effect of $[Fe(II)]_0$ on the degradation kinetics of BF by the Fenton-H_3NOH^+ (a) and the sole Fenton (b) processes, and dye elimination after 5 min (c) (vol. = 200 mL, pH 3, temp. ~25 °C, C_0 = 20 μM, $[Fe(II)]_0$ = 0.005–0.2 mM, $[H_2O_2]_0$ = 0.5 mM, $[H_3NOH^+]_0$ = 0.5 mM).

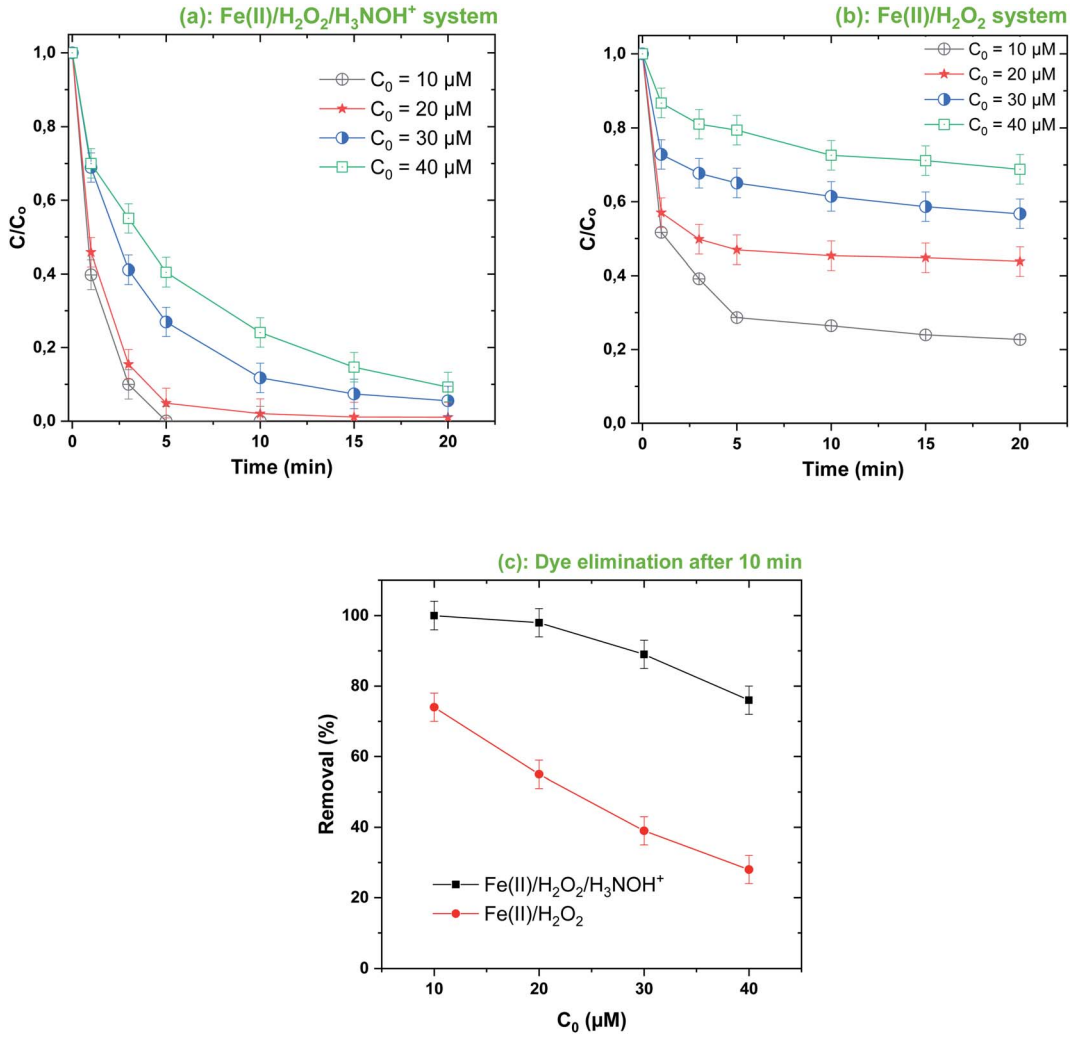

Fig. 7 Effect of initial dye concentration on its degradation kinetics by the Fenton-H_3NOH^+ (a) and the sole Fenton (b) processes, and dye elimination after 10 min (c) (vol. = 200 mL, pH 3, temp. ~25 °C, C_0 = 20–40 μM, $[Fe(II)]_0$ = 0.05 mM, $[H_2O_2]_0$ = 0.5 mM, $[H_3NOH^+]_0$ = 0.5 mM).

reactants resulted in different degrees of decrease in degradation efficiency. The effective quenching of reactive species, as shown in eqn (3) and (4), is one of the well-documented mechanisms for the inhibitory effects of utilizing high amounts of Fe(II) and H_2O_2. Furthermore, at higher Fe(II) and H_2O_2 concentrations, the amount of free radicals may be excessively high, favoring $^{\bullet}OH$ quenching by themselves (eqn (7), (14) and (15)) instead of their reaction with BF molecules. This behavior has been widely reported for a variety of degradation cases involving AOPs.[3,35,37,38,40,41] Consequently, iron(II) and H_2O_2 concentrations should be applied at optimized doses so as not to restrict the efficiency of the Fe(II)/H_2O_2/H_3NOH^+ integrated process.

The Fenton-H_3NOH^+ process is more efficient than the Fenton process over an extended interval of C_0 (10–40 μM), as depicted in Fig. 7a and b. The gap between removal curves with Fenton-H_3NOH^+ and Fenton increases from 26% at 10 μM to 43% at 20 μM and 50% at 30 and 40 μM (Fig. 7c). Therefore, the greater the concentration of contaminant, the greater the beneficial effect of hydroxylamine in the Fenton process. It should be noted that, even though the removal efficiency of BF in both processes decreased with the rise in C_0 (Fig. 7c), the reverse trend is recorded for the amount removed (in μM). For example, the amounts removed at C_0 = 10 μM are 7.4 and 10 μM for Fenton and Fenton-H_3NOH^+, respectively (ratio ~1.35). Amounts removed at C_0 = 40 μM became 11.2 and 30.4 μM for Fenton and Fenton-H_3NOH^+, respectively (ratio ~2.71). This trend, which was reported earlier for the degradation of different dyes by different AOPs,[27,38–40,46] clearly shows the positive effect of operating with a high BF concentration on its degradation efficiency, which is ascribed to the increased probability of oxidant attacks (hydroxyl radicals) upon BF molecules when the latter exist at a higher level. Besides, even though the dye removal kinetics in all Fenton-HA systems decrease exponentially (seeming to follow first-order kinetics), the first-order kinetics law is not applicable because the plot of the initial degradation rate of the dye *versus* its initial concentration (Fig. S1†) does not show a linear relationship as required for the first-order law ($r_{dye} = k[dye]$). The initial degradation rate increased with C_0 from 10 to 20 and then reached a plateau. The

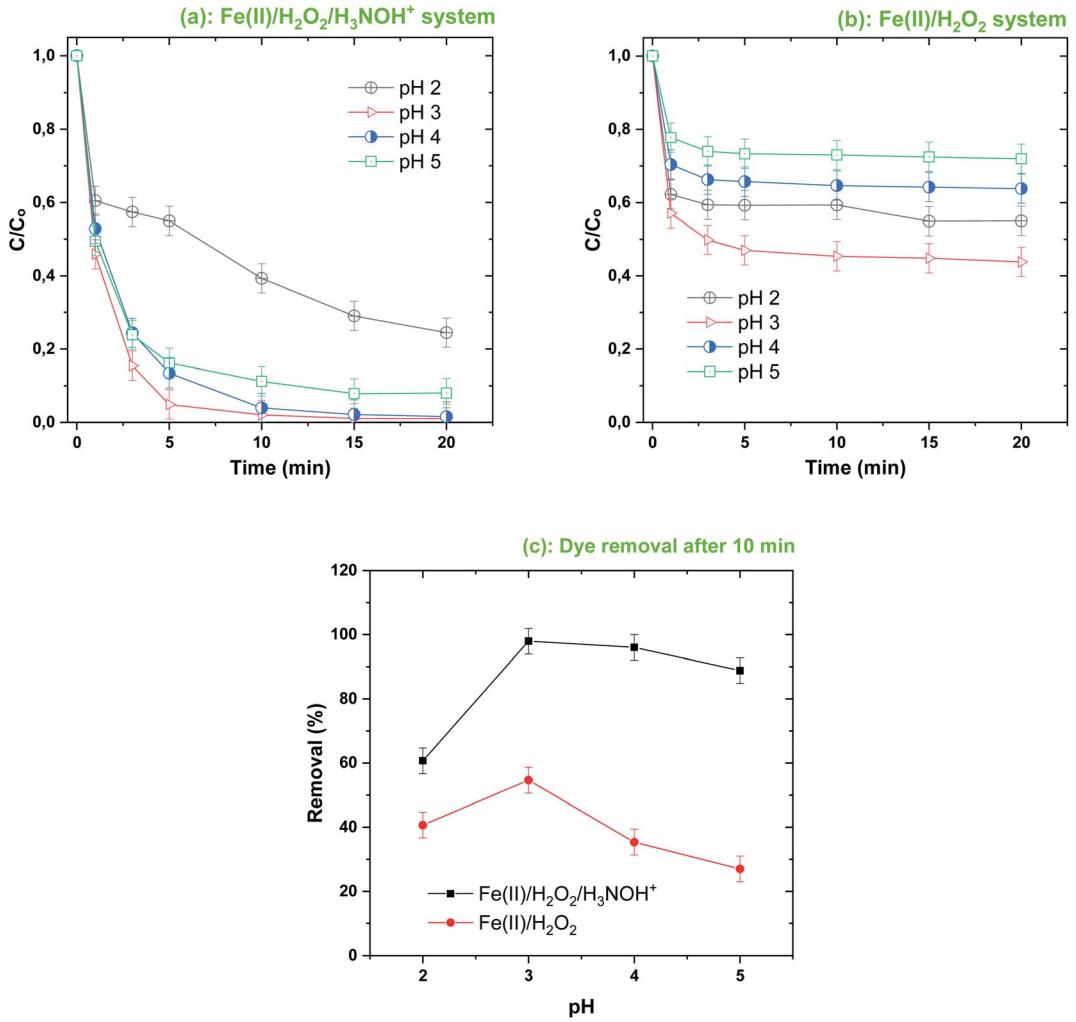

Fig. 8 Effect of initial solution pH on the degradation kinetics of BF by the Fenton-H_3NOH^+ (a) and the sole Fenton (b) processes, and dye elimination after 10 min (c) (vol. = 200 mL, pH 2–5, temp. ~25 °C, C_0 = 20 μM, $[Fe(II)]_0$ = 0.05 mM, $[H_2O_2]_0$ = 0.5 mM, $[H_3NOH^+]_0$ = 0.5 mM).

absence of a linear relationship implies that the degradation rate of the dye in the Fenton-HA system should not be analyzed based on a single rate constant (expressed in s^{-1}). This is the reason why all degradation kinetics throughout the manuscript have been analyzed by (i) the removal kinetics (C/C_0 *vs.* time) data for the Fenton and Fenton-HA degradation results (sub-figures b in Fig. 2, 5–8 and 11) and (ii) the removal efficiency at an advanced reaction time to compare the efficiency of the Fenton-HA process against the Fenton process (sub-figures c in Fig. 2, 5–8 and 11).

3.4. Effect of operating pH

Fig. 8 shows the effect of the initial solution pH (2–5) on the removal efficiency for BF (20 μM) with the Fenton-H_3NOH^+ and Fenton systems for fixed loadings of $[Fe(II)]_0$ = 0.05 mM and $[H_2O_2]_0 = [H_3NOH^+]_0$ = 0.5 mM. As shown in Fig. 8a, BF can be efficiently degraded in the Fenton-H_3NOH^+ system over a wide pH range from 3 to 5, with a comparable initial removal rate (~11 μM min^{-1}). For example, at pH 3 and 4, BF can be completely decomposed in ~15 min. When the initial reaction pH value was increased to 5, BF could also be efficiently degraded, when 92% of BF was degraded in 15 min. On the other hand, the efficiency of the Fenton process, which is already lower than that of Fenton coupled with hydroxylamine (previous sections), was greatly reduced by the elevation in pH, where maximum BF eliminations of 56, 36 and 29% were achieved at pH 3, 4 and 5, respectively. The ratio of BF removals with and without H_3NOH^+, as calculated from Fig. 7c, were 1.49, 1.79, 2.71 and 3.28 for a gradual increase in pH from 3 to 5 (in steps of one). Therefore, the best applicability of the hydroxylamine-assisted Fenton process is at pH 5, where a lower amount of acid is used but achieving a high degradation performance. However, above pH 5, a visible precipitate was detected for both processes (data not shown); a phenomenon which was not reported in previous studies treating several contaminants with the same integrated process.[17,25] Note that at pH 2, lower degradation efficiency was achieved compared to pH ≥ 3, either for Fenton or Fenton-assisted processes, even though the ternary system allows the best degradation yield to be achieved at a relatively advanced time (*i.e.*, 60.7% at 10 min), compared to 40% for the $Fe(II)/H_2O_2$ process (Fig. 8c). All the

above observations are in perfect agreement with those reported by Wang *et al.*[45] who studied the effect of the triple system Ce(IV)/H_2O_2/hydroxylamine for the degradation of Rhodamine. In Wang's results, pH 4 was considered the optimal pH for Rhodamine B degradation. The inhibition of BF degradation in a strongly acidic medium (pH 2), either with or without the addition of hydroxylamine (Fig. 8a and b), can be attributed to the presence of protons at high concentration, which inhibited the reaction of hydroxyl radicals with the dye molecules, as H^+ ions can scavenge $^{\cdot}OH$ through reaction (19) where electrons may be gained from ferrous ions.[45,47,48] In addition, the formation of electrophilic protonated H_2O_2 (*i.e.*, $H_3O_2^+$) *via* reaction (20) is another pathway that reduces the amount of one of the Fenton reagents in the solution.[45]

$$^{\cdot}OH + H^+ + e^- \rightarrow H_2O \quad (19)$$

$$H_2O_2 + H^+ \rightarrow H_3O_2^+ \quad (20)$$

On the other hand, since the pK_{a1} of hydroxylamine is 5.96,[16] hydroxylamine was found entirely in its protonated form, H_3NOH^+—which is less reactive toward $^{\cdot}OH$, as stated in the introduction by looking at the rate constants. Thus, the effect of pH on BF removal between pH 3 and 5 can mainly be attributed to the speciation of Fe(II) ions. In deionized water, the three species of Fe(II) with respect to pH are $Fe(H_2O)_6^{2+}$ or Fe^{2+}, which appear predominant in acidic conditions (pH $\leq$ 3); $Fe(H_2O)_4(OH)_2$ or $Fe(OH)_2$ at pH > 4; and $Fe(H_2O)_5(OH)^+$ and $FeOH^+$ coexisting at pH lower than 5. In these conditions, the concentration of $Fe(H_2O)_5(OH)^+$ is a maximum at around pH 3, whereas the precipitation of iron is important when the pH is above 3.[7] Thus, increasing the pH level above 3 could decrease the fraction of free Fe^{2+}, lowering the production of hydroxyl radicals through reaction (1). This is the most popular scenario elucidating the impact of pH on the efficiency of the Fenton process (Fig. 8b).[7,49] Iron speciation, on the other hand, is greatly influenced by a number of other factors, like ionic strength and total iron content.[50] The presence of electrolytes augments the ionic strength, causing iron precipitation to move to higher pH levels. An interesting discussion about this issue was given recently by Meghlaoui *et al.*[3] who found that pH 5 was the best value for the degradation of textile dyes in the Fe(II)/chlorine system. The authors revealed a displacement of iron speciation (precipitation) due to the presence of chlorine, as in

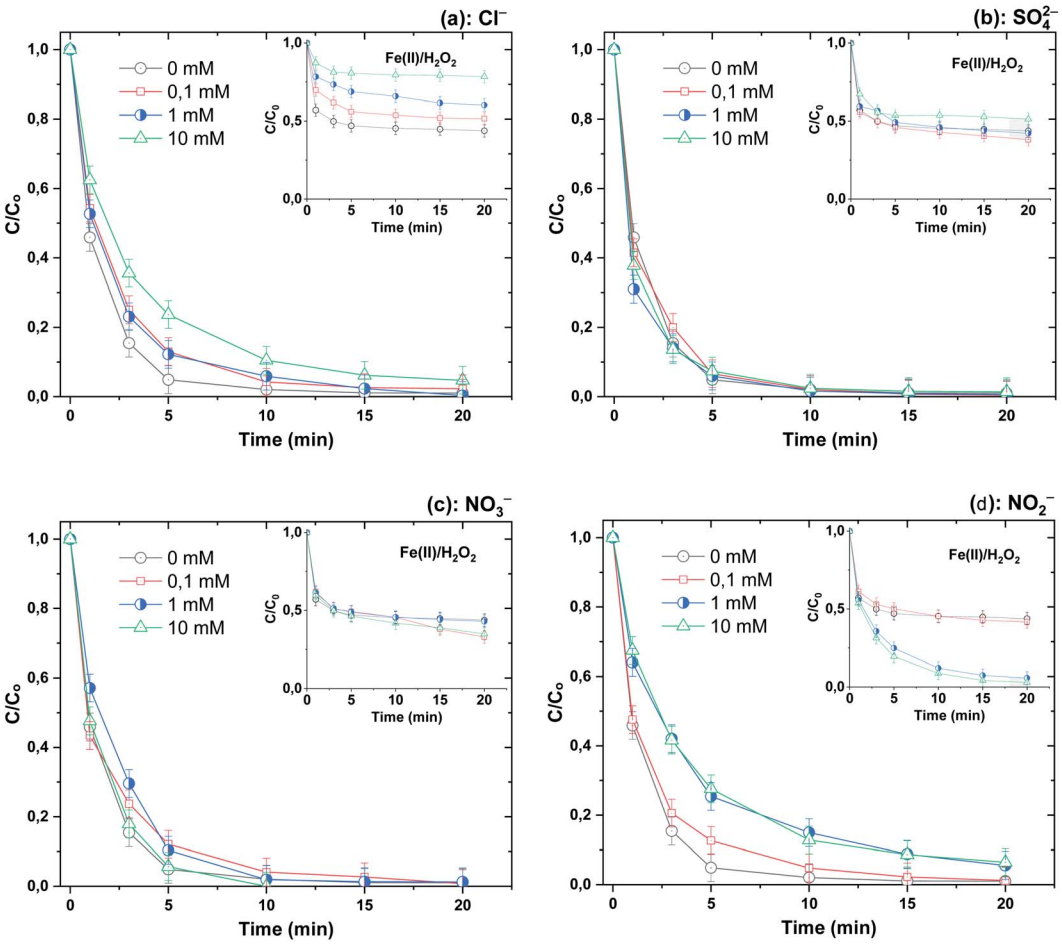

Fig. 9 Effect of different mineral anions (Cl^- (a), SO_4^{2-} (b), NO_3^- (c) and NO_2^- (d)) on the degradation kinetics of BF by the Fenton-H_3NOH^+ and the sole Fenton processes (vol. = 200 mL, pH 3, temp. ~25 °C, C_0 = 20 μM, $[Fe(II)]_0$ = 0.05 mM, $[H_2O_2]_0$ = 0.5 mM, $[H_3NOH^+]_0$ = 0.5 mM, $[anion]_0$ = 0–10 mM). The inserts show the degradation data through the Fenton process (without hydroxylamine).

some confirmed cases[51,52] reported and discussed by the authors.[3] Meghlaoui *et al.*, conclusion was that HClO/ClO^- may shift the dominance of Fe^{2+} ions up to a pH value higher than that reported for deionized water (*i.e.*, pH 3). This is presumably the scenario for our case where NH_3OH^+ may effectively move iron precipitation to higher pH value (but less than or equal to 5).

3.5. Effect of mineral anions and NOM

Because of the ubiquitous presence of mineral salts and natural organic matter (NOM) in surface water and real wastewater effluents,[53–55] we decided to test the impact of NaCl, Na_2SO_4, $NaNO_2$ and $NaNO_3$ (as sources of chloride, sulfate, nitrate and nitrite ions) and humic acids, as the main constituents of NOM,[55] on the performance of the Fe(II)/H_2O_2/NaH_3OH^+ ternary system toward the breakdown of BF (20 μM) at pH 3 using $[Fe(II)]_0 = 0.05$ mM and $[H_2O_2]_0 = [H_3NOH^+]_0 = 0.5$ mM. Fig. 8 depicts the impact of salts up to 10 mM, whereas Fig. 10 depicts the effect of NOM (5–20 mg L^{-1}). Salts have different impacts on process efficiency, depending on their concentration. While sulfate and nitrate did not influence the degradation processes, either in the presence or absence of H_3NOH^+ (Fig. 9b and c), chloride did. The degradation rate of BF was relatively decreased with the addition of Cl^-. For example, the removal of BF at 5 min decreased from 95% without Cl^- to 88 and 77% in the presence of 1 and 10 mM Cl^-, recording decreases of 7.3 and 18.9% in process efficiency, respectively (Fig. 9a). Nevertheless, low chloride concentration (<2 mM) has a marginal effect on dye removal kinetics, which is in accordance with the finding of Chen *et al.*[17] ($Cl^- = 0.4$ and 2 mM) for the degradation of benzoic acid at pH 3 in the presence of 0.4 mM H_3NOH^+. However, a more significant reduction effect of chloride ions is found in the Fenton process (no H_3NOH^+), where the maximum BF removal decreases from 54% with no Cl^- to 32 and 20% (40 and 62% reductions, respectively) in the presence of 1 and 10 mM Cl^- (Fig. 9a, inset). This observation is in agreement with that of Lu *et al.*[56] who also found the inhibition caused by chloride can be overcome by extending the reaction time at low concentrations. Peng *et al.*[19] reported that the presence of H_3NOH^+ accelerated the efficiency of the Fenton reagents toward the degradation of glycerin even in a hypersaline solution containing 5 M of NaCl. Chloride is usually known as a hydroxyl radical scavenger, where this reaction can yield less reactive oxidants ($Cl^{\bullet}$ and $Cl_2^{\bullet-}$) according to reactions (21)–(23).[57] The complexation of Fe(II)/Fe(III) with Cl^- through reactions (24)–(27) is another pathway that may cause a decline in oxidation efficiency *via* consumption of free iron.[19]

$$Cl^- + {}^{\bullet}OH \rightarrow ClOH^{\bullet-},\ k_{21} = 4.3 \times 10^9\ M^{-1}\ s^{-1} \quad (21)$$

$$ClOH^{\bullet-} \rightarrow Cl^{\bullet} + OH^-,\ k_{22} = 2.1 \times 10^{10}\ M^{-1}\ s^{-1} \quad (22)$$

$$Cl^{\bullet} + Cl^- \rightleftharpoons Cl_2^{\bullet-},\ k_{23} = (5.6\text{–}12) \times 10^9\ M^{-1}\ s^{-1},\ k_{-23} = (6\text{–}11) \times 10^4\ M^{-1}\ s^{-1} \quad (23)$$

$$Fe(II) + Cl^- \rightarrow FeCl^+ \quad (24)$$

$$FeCl^+ + Cl^- \rightarrow FeCl_2 \quad (25)$$

$$Fe(III) + Cl^- \rightarrow FeCl^{2+} \quad (26)$$

$$Fe(III) + 2Cl^- \rightarrow FeCl_2^+ \quad (27)$$

Note that at the lower dose of H_2O_2 (0.5 mM) used to test the effect of chlorine (Fig. 9a), the reaction between H_2O_2 and chloride is insignificant. This was confirmed by conducting a series of FB degradation runs in the system H_2O_2/Cl^- (with no iron or hydroxylamine). As shown in Fig. S2† of the SM, no significant change in the dye concentration is observed for chloride concentrations of 0.1 to 10 mM.

On the other hand, nitrite showed much more inhibition of BF degradation (Fig. 9d), where the dye removal at 5 min decreased from 95% in the absence of NO_2^- to 75% in the presence of 1 mM and no further inhibition was marked for an elevation in the concentration of the anion to 10 mM. This is due to the strong quenching of hydroxyl radicals by NO_2^- according to reaction (28), where the resulting $NO_2^{\bullet}$ is a less powerful oxidant than $^{\bullet}OH$.[44]

$$NO_2^- + {}^{\bullet}OH \rightarrow OH^- + NO_2^{\bullet},\ k_{28} = 1 \times 10^{10}\ M^{-1}\ s^{-1} \quad (28)$$

Surprisingly, the addition of nitrite in the absence of H_3NOH^+ accelerates the degradation rate of the dye (Fig. 9d, inset). The dye abatement becomes exponential, where near complete dye removal is achieved in 20 min for 1 and 10 mM of nitrite. These findings reveal that nitrite can interact with either Fe(II) or H_2O_2 to accelerate degradation. This issue necessitates additional research, which will be undertaken in forthcoming studies. The lack of further acceleration in the BF degradation rate when increasing nitrite doses from 1 to 10 mM can be

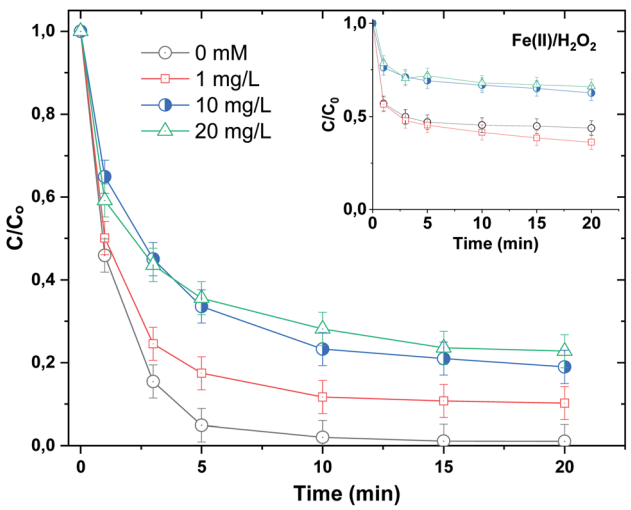

Fig. 10 Effect of humic acids (NOM) on the degradation kinetics of BF by the Fenton-H_3NOH^+ system (vol. = 200 mL, pH 3, temp. ~25 °C, C_0 = 20 μM, $[Fe(II)]_0 = 0.05$ mM, $[H_2O_2]_0 = 0.5$ mM, $[H_3NOH^+]_0 = 0.5$ mM, $[NOM]_0$ = 0–20 mg L^{-1}). The inset shows the degradation data through the Fenton process (without hydroxylamine).

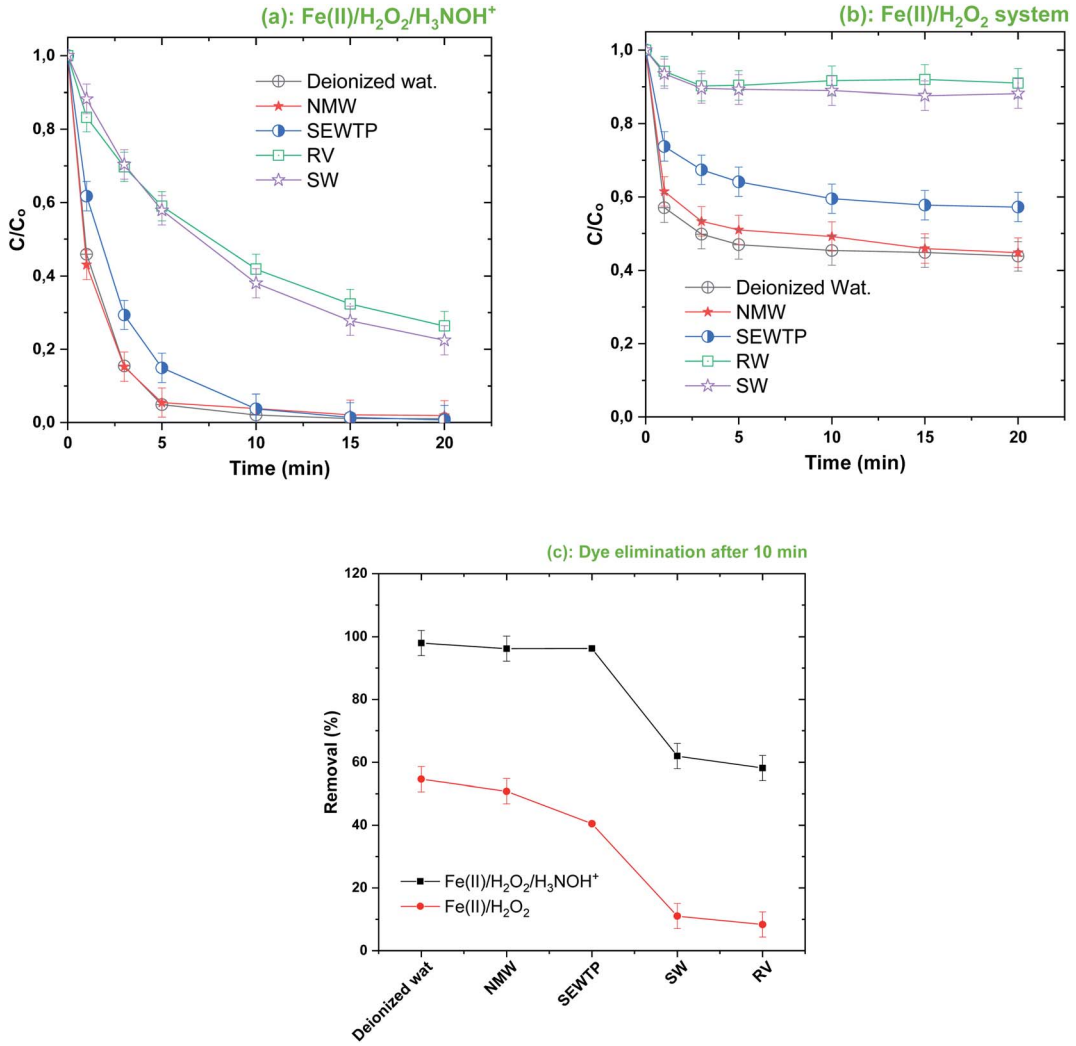

Fig. 11 Effect of water matrix quality on the degradation kinetics of BF by the Fenton-H_3NOH^+ (a) and the sole Fenton (b) processes, and dye elimination after 10 min (c) (vol. = 200 mL, pH 3, temp ~25 °C, $C_0 = 20$ μM, $[Fe(II)]_0 = 0.05$ mM, $[H_2O_2]_0 = 0.5$ mM, $[H_3NOH^+]_0 = 0.5$ mM). NMW: natural mineral water, SEWTP: secondary effluent from wastewater treatment plant, SW: seawater, RV: river water.

justified as in the case of an excess of H_3NOH^+, where $^{\bullet}OH$ quenching by NO_2^- (eqn (24)) becomes the dominant mechanism.

On the other hand, Fig. 10 demonstrates that the presence of NOM gradually diminished the degradation rate of BF upon $Fe(II)/H_2O_2/H_3NOH^+$ treatment; where removals of 92, 80 and 75% are achieved with 0, 1 and 10 mg L^{-1} of NOM, respectively (*i.e.*, yielding reductions of 13% for 1 mg L^{-1} and 18.4% for 10 mg L^{-1}). Correspondingly, NOM at 1 and 10 mg L^{-1} exerted a significant reduction in BF removal in the absence of H_3NOH^+ (Fig. 10, inset). Therefore, both processes are affected similarly by the presence of NOM. These outcomes, which are relatively well known regarding the impact of NOM on the performance of numerous $^{\bullet}OH$-based AOPs,[3,35,40,55] are ascribed to the quenching of hydroxyl radicals by NOM, in addition to the consumption of H_2O_2 reagent by NOM. The rate constant of the $^{\bullet}OH$-NOM reaction is 2.5×10^4 M^{-1} s^{-1}.[44] This relatively low rate constant justifies the insignificant reduction imposed by NOM at 10 mg L^{-1} compared to 1 mg L^{-1} (lower reactivity toward $^{\bullet}OH$) for the ternary system $Fe(II)/H_2O_2/H_3NOH^+$, as shown in Fig. 10.

3.6. Effect environmental matrices

Following the analysis of the effects of salts and NOM, the abatement of BF (20 μM) by the $Fe(II)/H_2O_2/H_3NOH^+$ integrated process was assessed in various water matrices (natural mineral water (NMW), river water, secondary effluents from a municipal wastewater treatment plant (SEWTP) and seawater (SW)). The achieved outcomes in the presence and absence of H_3NOH^+ are shown in Fig. 11. As can be seen, the ternary system maintained a higher degradation performance for the degradation of BF in NMW and SEWTP (Fig. 11a and c), which is principally ascribed to the lower salts and NOM loads in these matrices (see Table 1). Thus, a competitive scenario is not expected to be important in decreasing the degradation rate. The performance of the binary system (Fig. 11b) reveals the same tendency, except that of the

SEWTP which showed a relatively greater reduction than the case of the ternary oxidation system, as can clearly be seen in Fig. 11c. However, the degradation efficiency is greatly diminished in seawater and river water, where only 61 and 58% of BF were removed after 10 min, respectively (compared to 98% in deionized water). For the Fenton process (Fig. 11b), the reduction is more remarkable; the dye removal being 11 and 8% in both matrices, instead 54% for pure water, which marks 79 and 85% reductions in the respective matrices. This fact is due to the high load of salts in the seawater (salinity 35 g L^{-1}) and NOM in river water (Table 1), which provokes severe competition to react with hydroxyl radicals, as stated in the earlier sections. River water also contains micro-colloids (existing even after filtration) which cause an effective alteration in BF oxidation through consuming Fe(II) ions (ferrous ions are usually used as coagulants in water treatment for removing negatively charged micro-colloids existing in surface waters). In the seawater, not only can Cl^- scavenge $^{\bullet}OH$ but so can bromide ions which also exist in significant amounts (65–80 mg L^{-1}, Table 1). Br^- is an efficient $^{\bullet}OH$-scavenger according to reactions (29)–(32).[44,57] The contribution of the resulting bromide-containing radicals is not significant compared to that of $^{\bullet}OH$, by reason of the highly reactive character of the latter.[57]

$$Br^- + {}^{\bullet}OH \rightleftharpoons BrOH^{\bullet -},\ k_{29} = 1.1 \times 10^{10}\ M^{-1}\ s^{-1},\ k_{-29} = 3.3 \times 10^{7}\ M^{-1}\ s^{-1} \quad (29)$$

$$BrOH^{\bullet -} \rightarrow Br^{\bullet} + OH^-,\ k_{30} = 1.9 \times 10^{8}\ M^{-1}\ s^{-1} \quad (30)$$

$$BrOH^{\bullet -} + Br^- \rightarrow Br^{\bullet} + OH^-,\ k_{31} = 4.4 \times 10^{10}\ M^{-1}\ s^{-1} \quad (31)$$

$$Br^{\bullet} + Br^- \rightleftharpoons Br_2^{\bullet -},\ k_{32} = 1.2 \times 10^{10}\ M^{-1}\ s^{-1},\ k_{-32} = 10^{5}\ M^{-1}\ s^{-1} \quad (32)$$

Note that the difference in BF removal efficiency, as calculated from Fig. 10c, is always between 40 and 50%, translating the significant impact of H_3NOH^+ where it assists the Fenton reagents in the degradation of refractory textile dyes whatever the composition of the water matrices.

4. Conclusions

This investigation revealed that the degree of hydroxylamine-induced acceleration of the Fenton process depends on operating circumstances and water quality. The first and most important parameter is pH, which is restricted to pH 5 where only the protonated form (H_3NOH^+) of hydroxylamine can effectively convert Fe(III) into Fe(II) without considerable quenching of the hydroxyl radical ($k_{\cdot OH,H3NOH^+} \leq 5.0 \times 10^8\ M^{-1}\ s^{-1}$). Greater degradation rates were associated with higher initial H_3NOH^+, Fe(II) and H_2O_2 doses; however, optimum degradation points were observed for H_3NOH^+ and Fe(II) in the Fenton-H_3NOH^+ system, where excessive additions of these reagents quench radical formation in the dye solution. The difference between the Fenton-H_3NOH^+ and Fenton systems in terms of dye removal efficiency increases with increasing reactants (*i.e.*, H_3NOH^+, H_2O_2, Fe(II) and dye) dosages and solution pH (2–5). Nitrite addition (which reduced the Fenton-H_3NOH^+ efficiency) notably accelerated the efficiency of the Fenton reaction, suggesting that NO_2^- can act as an intensifier of the Fenton process; this statement will be tested in further future investigations. The dye (BF) degradation efficiency in the presence of H_3NOH^+ is much higher (as in deionized water) in natural mineral water and secondary effluent from a wastewater treatment plant; however, significant losses in process efficiency were remarked in seawater and river water, due to the high contents in these two matrices of salts and NOM (*i.e.*, radical scavengers).

Eventually, the degree to which the Fenton-H_3NOH^+ process reduces the organic load (TOC, COD and BOD analyses) and the effluent toxicity will be studied in forthcoming work. Furthermore, additional investigations, such as the identification of degradation by-products and nitrogenous species (NO_2^-, NO_3^-…), resulting from hydroxylamine reduction, is still required for the feasibility of the process. Correspondingly, printing and dyeing wastewater contains a lot of organic matter, such as dyes, starch, cellulose, lignin, detergents, *etc.* These organic matters could of course alter the process efficiency through radical consumption, like the case of river water where the natural organic matters have provoked a massive reduction in process efficiency. The feasibility of the integrated process for treating real samples of dyeing wastewater (all with process optimization) will be verified in future investigations. Finally, determining the speciation of the Fe(II)/H_2O_2/H_3NOH^+ ternary system related to loadings of different reactants is an essential perspective of this project. The determination of this diagram of speciation allows answers to several complicated issues like extending the operating pH up to 5 with no precipitation of iron.

Conflicts of interest

There are no conflicts to declare.

Acknowledgements

This study was supported by The Ministry of Higher Education and Scientific Research of Algeria (project No. A16N01UN250320180001) and the General Directorate of Scientific Research and Technological Development (GD-SRTD) of Algeria.

References

1 F. Ghanbari and M. Moradi, in *Advanced Nanomaterials for Wastewater Remediation*, ed. Ravindra Kumar Gautam and M. C. Chattopadhyaya, Boca Raton, CRC Press, 2016.
2 F. Ghanbari and M. Moradi, *Advanced Nanomaterials for Wastewater Remediation Ch_3 (Electrooxidation Processes for Dye Degradation and Colored Wastewater Treatment)*, 2022.
3 F. Z. Meghlaoui, S. Merouani, O. Hamdaoui, M. Bouhelassa and M. Ashokkumar, Rapid catalytic degradation of refractory textile dyes in Fe (II)/chlorine system at near neutral pH: Radical mechanism involving chlorine radical

anion (Cl2˙−)-mediated transformation pathways and impact of environmental matrices, *Sep. Purif. Technol.*, 2019, **227**, 115685.

4 H. J. H. Fenton, Oxidation of tartaric acid in presence of iron, *J. Chem. Soc. Trans.*, 1894, **65**, 899–910.

5 F. Haber and J. Weiss, The catalytic decomposition of hydrogen peroxide by iron salts, *Proc. R. Soc. London. Ser. A, Math. Phys. Sci.*, 1934, **147**, 332–351.

6 Y. Li and H. Cheng, Chemical kinetic modeling of organic pollutant degradation in Fenton and solar photo-Fenton processes, *J. Taiwan Inst. Chem. Eng.*, 2021, **123**, 175–184.

7 J. J. Pignatello, E. Oliveros and A. MacKay, Advanced oxidation processes for organic contaminant destruction based on the fenton reaction and related chemistry, *Crit. Rev. Environ. Sci. Technol.*, 2006, **36**, 1–84.

8 F. C. Moreira, R. A. R. Boaventura, E. Brillas and V. J. P. Vilar, Electrochemical advanced oxidation processes: A review on their application to synthetic and real wastewaters, *Appl. Catal. B Environ.*, 2017, **202**, 217–261.

9 E. Brillas, I. Sirés and M. A. Oturan, Electro-Fenton process and related electrochemical technologies based on Fenton's reaction chemistry, *Chem. Rev.*, 2009, **109**, 6570–6631.

10 E. Brillas and C. A. Martínez-huitle, Decontamination of wastewaters containing synthetic organic dyes by electrochemical methods. An updated review, *Appl. Catal. B Environ.*, 2015, **166–167**, 603–643.

11 V. A. B. Paiva, C. E. S. Paniagua, I. A. Ricardo, B. R. Gonçalves, S. P. Martins, D. Daniel, A. E. H. Machado and A. G. Trovó, Simultaneous degradation of pharmaceuticals by classic and modified photo-Fenton process, *J. Environ. Chem. Eng.*, 2018, **6**, 1086–1092.

12 R. D. Villa, A. G. Trovó and R. F. P. Nogueira, Environmental implications of soil remediation using the Fenton process, *Chemosphere*, 2008, **71**, 43–50.

13 E. Mousset, C. Trellu, N. Oturan, M. A. Rodrigo and M. A. Oturan, in *Electro-Fenton Process. The Handbook of Environmental Chemistry*, ed. M. Zhou, M. Oturan and I. Sirés, Springer, Singapore, 2017, vol. 61.

14 G. V. Buxton, C. L. Greenstock, W. P. Helman and A. B. Ross, Critical review of rate constants for reactions of hydrated Electrons, hydrogen atoms and hydroxyl radicals (˙OH/O-) in aqueous solution, *J. Phys. Chem. Ref. Data*, 1988, **17**, 515–886.

15 M. Sillanpaa, M. C. Ncibi and A. Matilainen, Advanced oxidation processes for the removal of natural organic matter from drinking water sources: A comprehensive review, *J. Environ. Manage.*, 2018, **208**, 56–76.

16 L. Chen, X. Li, J. Zhang, J. Fang, Y. Huang, P. Wang and J. Ma, Production of hydroxyl radical via the activation of hydrogen peroxide by hHydroxylamine, *Environ. Sci. Technol.*, 2015, **49**, 10373–10379.

17 L. Chen, J. Ma, X. Li, J. Zhang, J. Fang, Y. Guan and P. Xie, Strong enhancement on Fenton oxidation by addition of hydroxylamine to accelerate the Ferric and Ferrous iron cycles, *Environ. Sci. Technol.*, 2011, **45**, 3925–3930.

18 Z. Y. Li, L. Wang, Y. L. Liu, Q. Zhao and J. Ma, Unraveling the interaction of hydroxylamine and Fe(III) in Fe(II)/Persulfate system: A kinetic and simulating study, *Water Res.*, 2020, **168**, 115093.

19 S. Peng, W. Zhang, J. He, X. Yang, D. Wang and G. Zeng, Enhancement of Fenton oxidation for removing organic matter from hypersaline solution by accelerating ferric system with hydroxylamine hydrochloride and benzoquinone, *J. Environ. Sci.*, 2016, **41**, 16–23.

20 Z. Bu, X. Li, Y. Xue, J. Ye, J. Zhang and Y. Pan, Hydroxylamine enhanced treatment of highly salty wastewater in Fe0/H2O2 system : Efficiency and mechanism study, *Sep. Purif. Technol.*, 2021, **271**, 118847.

21 G. Liu, X. Li, B. Han, L. Chen, L. Zhu and L. C. Campos, Efficient degradation of sulfamethoxazole by the Fe(II)/HSO5− process enhanced by hydroxylamine: Efficiency and mechanism, *J. Hazard. Mater.*, 2017, **322**, 461–468.

22 J. Zou, J. Ma, L. Chen, X. Li, Y. Guan, P. Xie and C. Pan, Rapid acceleration of ferrous Iron/peroxymonosulfate oxidation of organic pollutants by promoting Fe(III)/Fe(II) cycle with hydroxylamine, *Environ. Sci. Technol.*, 2013, **47**, 11685–11691.

23 G. Bengtsson, S. Fronæus and L. Bengtsson-Kloo, The kinetics and mechanism of oxidation of hydroxylamine by iron(III), *J. Chem. Soc. Dalt. Trans.*, 2002, **12**, 2548–2552.

24 J. Duan, S. Pang, Z. Wang, Y. Zhou, Y. Gao and J. Li, Hydroxylamine driven advanced oxidation processes for water treatment : A review, *Chemosphere*, 2021, **262**, 128390.

25 C. Wang, G. Yu, H. Chen and J. Wang, Degradation of norfloxacin by hydroxylamine enhanced fenton system: Kinetics, mechanism and degradation pathway, *Chemosphere*, 2021, **270**, 129408.

26 S. Merouani, O. Hamdaoui, F. Saoudi and M. Chiha, Sonochemical degradation of Rhodamine B in aqueous phase: Effects of additives, *Chem. Eng. J.*, 2010, **158**, 550–557.

27 H. Bendjama, S. Merouani, O. Hamdaoui and M. Bouhelassa, UV-photolysis of Chlorazol Black in aqueous media: Process intensification using acetone and evidence of methyl radical implication in the degradation process, *J. Photochem. Photobiol. A Chem.*, 2019, **368**, 268–275.

28 S. Merouani, O. Hamdaoui and M. Bouhelassa, Degradation of Safranin O by thermally activated persulfate in the presence of mineral and organic additives : impact of environmental matrices, *Desalin. Water Treat.*, 2017, **75**, 202–212.

29 A. Taamallah, S. Merouani and O. Hamdaoui, Sonochemical degradation of basic fuchsin in water, *Desalin. Water Treat.*, 2016, **57**, 27314–27330.

30 A. Haddad, S. Merouani, C. Hannachi, O. Hamdaoui and B. Hamrouni, Intensification of light green SF yellowish (LGSFY) photodegradion in water by iodate ions: Iodine radicals implication in the degradation process and impacts of water matrix components, *Sci. Total Environ.*, 2019, **652**, 1219–1227.

31 S. Merouani, O. Hamdaoui, F. Saoudi and M. Chiha, Influence of experimental parameters on sonochemistry

dosimetries: KI oxidation, Fricke reaction and H2O2 production, *J. Hazard. Mater.*, 2010, **178**, 1007–1014.
32 S. Wang and J. Wang, Trimethoprim degradation by Fenton and Fe(II)-activated persulfate processes, *Chemosphere*, 2018, **191**, 97–105.
33 H. J. Hsing, P. C. Chiang, E. E. Chang and M. Y. Chen, The decolorization and mineralization of Acid Orange 6 azo dye in aqueous solution by advanced oxidation processes: A comparative study, *J. Hazard. Mater.*, 2007, **141**, 8–16.
34 B. Kayan, B. Gözmen, M. Demirel and A. M. Gizir, Degradation of acid red 97 dye in aqueous medium using wet oxidation and electro-Fenton techniques, *J. Hazard. Mater.*, 2010, **177**, 95–102.
35 S. Bekkouche, S. Merouani, O. Hamdaoui and M. Bouhelassa, Efficient photocatalytic degradation of Safranin O by integrating solar-UV/TiO2/persulfate treatment: Implication of sulfate radical in the oxidation process and effect of various water matrix components, *J. Photochem. Photobiol. A Chem.*, 2017, **345**, 80–91.
36 O. Hamdaoui and S. Merouani, Improvement of sonochemical degradation of brilliant blue R in water using periodate ions: Implication of iodine radicals in the oxidation process, *Ultrason. Sonochem.*, 2017, **37**, 344–350.
37 H. Ferkous, S. Merouani, O. Hamdaoui and C. Pétrier, Persulfate-enhanced sonochemical degradation of naphthol blue black in water: Evidence of sulfate radical formation, *Ultrason. Sonochem.*, 2017, **34**, 580–587.
38 N. E. Chadi, S. Merouani, O. Hamdaoui, M. Bouhelassa and M. Ashokkumar, H2O2/Periodate (IO4−): A novel advanced oxidation technology for the degradation of refractory organic pollutants, *Environ. Sci. Water Res. Technol.*, 2019, **5**, 1113–1123.
39 F. Z. Meghlaoui, S. Merouani, O. Hamdaoui, A. Alghyamah, M. Bouhelassa and M. Ashokkumar, Fe(III)-catalyzed degradation of persistent textile dyes by chlorine at slightly acidic conditions: the crucial role of Cl2•− radical in the degradation process and impacts of mineral and organic competitors, *Asia-Pacific J. Chem. Eng.*, 2020, 1–12.
40 A. A. Belghit, S. Merouani, O. Hamdaoui, M. Bouhelassa, A. Alghyamah and M. Bouhelassa, Influence of processing conditions on the synergism between UV irradiation and chlorine toward the degradation of refractory organic pollutants in UV/chlorine advanced oxidation system, *Sci. Total Environ.*, 2020, **736**, 139623_1–139623_10.
41 H. Bendjama, S. Merouani, O. Hamdaoui and M. Bouhelassa, Efficient degradation method of emerging organic pollutants in marine environment using UV/periodate process: Case of chlorazol black, *Mar. Pollut. Bull.*, 2018, **126**, 557–564.
42 S. N. A. Shah, H. Li and J. M. Lin, Enhancement of periodate-hydrogen peroxide chemiluminescence by nitrogen doped carbon dots and its application for the determination of pyrogallol and gallic acid, *Talanta*, 2016, **153**, 23–30.
43 Z. Wei, F. A. Villamena and L. K. Weavers, Kinetics and Mechanism of Ultrasonic Activation of Persulfate: An in Situ EPR Spin Trapping Study, *Environ. Sci. Technol.*, 2017, **51**, 3410–3417.
44 A. Belghit, S. Merouani, O. Hamdaoui, M. Bouhelassa and S. Al-Zahrani, The multiple role of inorganic and organic additives in the degradation of reactive green 12 by UV/chlorine advanced oxidation process, *Environ. Technol.*, 2020, 1–27, in press.
45 S. Wang, Y. Jia, L. Song and H. Zhang, Decolorization and mineralization of Rhodamine B in aqueous solution with a triple system of Cerium(IV)/H2O2/Hydroxylamine, *ACS Omega*, 2018, **3**, 18456–18465.
46 H. Ferkous, O. Hamdaoui and S. Merouani, Sonochemical degradation of naphthol blue black in water: Effect of operating parameters, *Ultrason. Sonochem.*, 2015, **26**, 40–47.
47 W. Z. Tang and C. P. Huang, 2,4-Dichlorophenol oxidation kinetics by Fenton's reagent, *Environ. Technol.*, 1996, **17**, 1371–1378.
48 L. G. Devi, K. E. Rajashekhar, K. S. A. Raju and S. G. Kumar, Kinetic modeling based on the non-linear regression analysis for the degradation of Alizarin Red S by advanced photo Fenton process using zero valent metallic iron as the catalyst, *J. Mol. Catal. A Chem.*, 2009, **314**, 88–94.
49 A. D. Bokare and W. Choi, Review of iron-free Fenton-like systems for activating H2O2in advanced oxidation processes, *J. Hazard. Mater.*, 2014, **275**, 121–135.
50 M. I. Polo-López, S. Nahim-Granados and P. Fernández-Ibáñez, Homogeneous Fenton and Photo-Fenton Disinfection of Surface and Groundwater, in *Applications of Advanced Oxidation Processes (AOPs) in Drinking Water Treatment (The Handbook of Environmental Chemistry)*, ed. A. Gil, L. Galeano and M. Vicente, Springer, Cham, 2018, vol. 67, pp. 155–177.
51 D. W. King, Role of Carbonate Speciation on the Oxidation Rate of Fe(II) in Aquatic Systems, *Environ. Sci. Technol.*, 1998, **32**, 2997–3003.
52 F. J. Millero, W. Yao and J. Aicher, The speciation of Fe(II) and Fe(III) in natural waters, *Mar. Chem.*, 1995, **50**, 21–39.
53 L. K. Weavers, G. Y. Pee, J. A. Frim, L. Yang, J. F. Rathman, L. K. Weavers, G. Y. Pee, J. A. Frim, L. Yang and J. F. Rathman, Ultrasonic destruction of surfactants: Application to industrial wastewaters, *Water Environ. Reasearch*, 2005, **77**, 259–265.
54 M. P. Rayaroth, U. K. Aravind and C. T. Aravindakumar, Sonochemical degradation of Coomassie Brilliant Blue: Effect of frequency, power density, pH and various additives, *Chemosphere*, 2015, **119**, 848–855.
55 O. Hamdaoui and S. Merouani, Ultrasonic destruction of acid Orange 7 : Effect of humic acid, surfactants and complex matrices, *Water Environ. Reasearch*, 2017, **89**, 250–259.
56 M. C. Lu, Y. F. Chang, I. M. Chen and Y. Y. Huang, Effect of chloride ions on the oxidation of aniline by Fenton's reagent, *J. Environ. Manage.*, 2005, **75**, 177–182.
57 N. E. Chadi, S. Merouani, O. Hamdaoui, M. Bouhelassa and M. Ashokkumar, Influence of mineral water constituents, organic matter and water matrices on the performance of the H2O2/IO4–advanced oxidation process, *Environ. Sci. Water Res. Technol.*, 2019, **5**, 1985–1992.